A Method for the Determination of Balance Coefficient and Elevator Braking Torque in a Tower Parking Car System

Truong Giang Duong
Faculty of Mechanical Engineering, Hanoi University of Civil Engineering, Vietnam
giangdt@huce.edu.vn (corresponding author)

Received: 25 September 2023 | Revised: 15 October 2023 | Accepted: 1 November 2023

 DOI: https://doi.org/10.48084/etasr.6439

ABSTRACT

Multistory car parking systems are a solution that brings many benefits, especially in urban areas as the number of cars increases. This study investigated the elevator of a multistory car parking system to determine the balance coefficient to reduce driving power and the influence on braking torque. The parameters were calculated based on the establishment of a planning matrix and using the calculation tools and the Taguchi method in the Minitab software. A formula was developed to calculate the braking torque of an elevator, considering the coefficient of the balancing system to ensure optimal driving power. The balance coefficient and the necessary braking torque were determined and the power was reduced by 17.5% while the braking torque was increased by 13.4% compared to the conventional method.

Keywords-counterweight; balance coefficient; brake torque; parking car system; optimal driving power

I. INTRODUCTION

As the number of cars increases and there are fewer and fewer parking spaces, the city traffic increases [1]. Therefore, research on multistory car parking systems is necessary [2-4]. Multistory parking car systems are a solution that brings many benefits, especially in urban areas. Many studies investigated parking types and multistory car parking systems, conducted kinematic and dynamic analyses, and applied finite element methods [3-4]. In [5], two automatic systems were investigated to find the causes of accidents and damage. In [6], the dynamics of the freight elevators were analyzed to find the acceleration of the movement and propose recommendations to increase efficiency. In [7] a similar problem was investigated, which is the dynamic analysis of vertical transport machines in mining.

In [8-12], some structural solutions for parking car systems were proposed. In [8], a mechanical device was proposed for a multi-story parking system using a lift table. This type of lifting structure has the advantage of not needing anti-sway guidance when lifting but has the disadvantage of a limited lifting height. The invention in [8] also used a self-propelled table-type lifting device running underneath to load the vehicle. This type of system structure is suitable for basements with limited transport height. The invention in [10] is a multistory parking solution with 2 entry and exit lanes, and each module has an independent lift to load and unload cars vertically. This has the advantage of a fast vehicle loading time and the disadvantage of having to arrange many elevators. In addition, it does not arrange a balancing system when the lifting height is large, thus affecting the engine's driving power. The multistory parking car tower in [11] is a structure that uses a central elevator and the counterweights of the balancing system are inserted into the guide columns. This type of structure is suitable for height development due to the balanced system arrangement, but the number of cars on one floor is limited. In [12], a pallet locking system was proposed, which is used to lock car parking pallets with or without vehicles in a multistory car parking system.

Figure 1 describes the structure of a tower car parking system, with a lifting mechanism used to raise and lower the sliding frame to the corresponding floors. The counterweight and the cable are part of the elevator balance system. This system balances the weights of the sliding frame and the vehicle. The counterweight moves inside the guide column. The proposed design option, shown in Figure 1, allows transport to high altitudes, saving energy due to the balanced arrangement of the system. In addition, the elevator allows for winch transport to multiple parking locations on each floor. In [13], a method was proposed to determine the weight of the cabin and the counterweight of the elevator balancing system. However, this study did not mention the influence of the braking torque or the method for determining it. The load carrying capacity and the weight of the counterweight and the cabin when unloaded are the technical basis for calculating the balance coefficient of the elevator, which is obtained by dividing the difference between the total weight of the counterweight device and the car when unloaded by the rated load capacity of the elevator. In [14-15], it was proposed that the balance coefficient of passenger elevators should be from 0.4 to 0.5. Therefore, the balance coefficient for elevators in multistory car parking systems does not have capacity optimization guidelines such as passenger elevators.

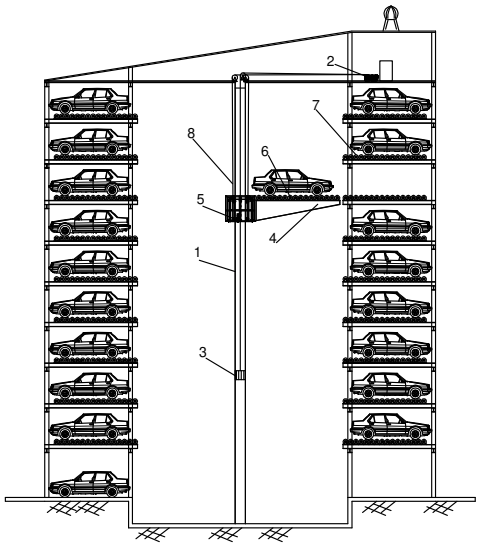

Fig. 1. Tower car parking system: 1. Sliding guide column, 2. Winches, 3. Counterweight, 4. Sliding frame, 5. Rotating mechanism, 6-7. Car push and pull system, 8. Cable.

The choice of the drive diagram and the weight of the components of the balancing system, in addition to greatly affecting the driving power, also affect the required braking torque. Moreover, the braking time and distance need to be guaranteed. This study aimed to determine the counterweight through the balance coefficient to ensure optimal driving power. Then the expression for calculating the elevator braking torque was established, taking into account the factors of the balancing system. The experimental research method calculated the parameters based on a planning matrix, the Taguchi method, and the Minitab software. The Taguchi method was also used in [16-19]. The results of the study helped determine the balance coefficient and the braking torque required according to the optimal power of elevators in tower car parking systems.

II. CALCULATION METHOD

A. Power and Balance Coefficient

There are two specific working states of the elevator, including the full load case, braking when lowering the slide frame at the bottom (Figure 2(a)), and the unloaded case, braking when lowering the counterweight at the bottom (Figure 2(b)). Ignoring the auxiliary forces, the dynamic load components, and the weight of the lifting cable, the unbalanced weight in the case of a load is (G_1+G_2-G_3). The unbalanced weight in the unloaded case is (G_3-G_2). When considering the unbalanced weight in two equal cases, the following equation arises:

$$G_3 = 0.5G_1 + G_2 \quad (1)$$

where G_1 is the weight of the car (N), G_2 is the weight of the sliding frame (N), and G_3 is the weight of the counterweight (N). In calculating passenger elevators, the weight counterweight is determined by the balance coefficient ψ [14-15]. The weight of the counterweight is given by:

$$G_3 = G_2 + \psi G_1 \quad (2)$$

where ψ is the balance coefficient. In the design of passenger elevators, the balance coefficient ψ is in the range of 0.4 - 0.5 [14-15]. In a multi-story parking car system, the weight of the car varies according to its type, but the difference is not much.

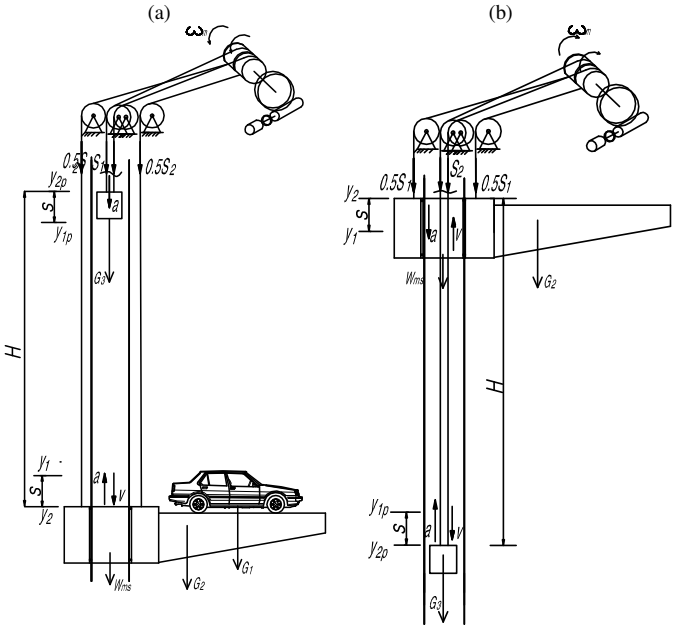

Fig. 2. Calculation diagrams: (a) in the case of full load, brake when lowering the sliding frame at the bottom, (b) in the case of no load, brake when lowering the counterweight at the bottom.

When excluding the effect of dynamic load, in the case of full load and braking when lowering the sliding frame at the bottom, the power is calculated according to (3). In the case of no load and braking when lowering the counterweight at the bottom, the power is calculated according to (4):

$$N_1 = \frac{S_2 - S_1}{1000\eta} v = \frac{W_{ms} + \gamma H g + G_1(1-\psi)}{1000\eta} v \quad (3)$$

$$N_2 = \frac{S_2 - S_1}{1000\eta} v = \frac{\psi G_1 + \gamma H g - W_{ms}}{1000\eta} v \quad (4)$$

where S_1 is the small tension force (N), S_2 is the large tension force (N), v is the lifting or lowering speed (m/s), γ is the cable density per meter (kg/m), g is the gravitational acceleration (m/s^2), W_{ms} are the auxiliary barrier components (N), H is the design lifting height (m), and η is the system's performance.

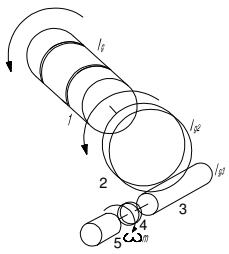

Fig. 3. Drive diagram of the winch: 1. Friction drum, 2. Screw wheel, 3. Screw shaft, 4. Brake, 5. Motor.

B. Determining the Braking Torque while taking into Account the Balancing System Factors

In the general case of braking when lowering the sliding frame with full load (Figure 2(a)), the mechanism driving diagram is shown in Figure 3. Kinetic energy ΔKE is determined by:

$$\Delta KE = \left(\frac{I_d}{2i_{23}^2} + \frac{I_{g2}}{2i_{23}^2} + \frac{I_{g3} + I_{g4} + I_5}{2}\right)\omega_m^2 + \frac{(G_1 + G_2)v^2}{2g} + \frac{\gamma H v^2}{2g} - \frac{(G_2 + \psi G_1)v^2}{2g} \quad (5)$$

where I_{g2} and I_{g3} are the moments of inertia of worm gear 2 and worm shaft 3 (kgm^2), I_{g4} and I_{g5} are the moments of inertia of the brake wheel and engine rotor (kgm^2), I_d is the drum moment of inertia (kgm^2), i_{23} is the transmission ratio, and ω_m is the angular velocity at the brake axis (rad/s).

The potential energy ΔPE_r of the cable suspending the load when it changes position from $y_1 = H - s$ to $y_2 = H$ is determined by:

$$\Delta PE_r = \gamma g \int_{y_1}^{y_2} y dy = \frac{\gamma g}{2}[H^2 - (H - s)^2] \quad (6)$$

where s is the braking distance, and y is the position of the considered part (m). The potential energy ΔPE_{rp} of the counterweight suspension cable when it changes position from $y_{1p} = s$ to $y_{2p} = 0$ is given by:

$$\Delta PE_{rp} = \gamma g \int_{y_{1p}}^{y_{2p}} y dy = -\frac{\gamma g}{2} s^2 \quad (7)$$

The potential energy ΔPE of the system in Figure 2(a) is represented by:

$$\Delta PE = (G_1 + G_2)s + \frac{\gamma g}{2}[H^2 - (H - s)^2] - (G_2 + \psi G_1)s - \frac{\gamma g}{2} s^2 \quad (8)$$

The movement of sliding frame 4 and counterweight 3 (Figure 1) is in the vertical direction, so the energy change due to braking is the sum of changes in kinetic and potential energy and other work on the system. Therefore, the energy change ΔE (N/m) can be written as:

$$\Delta E = \Delta KE + \Delta PE + \Delta W_{ms} \quad (9)$$

where ΔW_{ms} is the input to the system due to secondary resistances. Substituting into (9):

$$\Delta E = \left(\frac{I_d}{2i_{23}^2} + \frac{I_{g2}}{2i_{23}^2} + \frac{I_{g3} + I_{g4} + I_5}{2}\right)\omega_m^2 + \frac{(G_1 + G_2)v^2}{2g} + \frac{\gamma H v^2}{2g} - \frac{(G_2 + \psi G_1)v^2}{2g} + (G_1 + G_2)s + \frac{\gamma g}{2}[H^2 - (H - s)^2] - (G_2 + \psi G_1)s - \frac{\gamma g}{2} s^2 - W_{ms} s \quad (10)$$

Assuming rotation speed from the initial value ω_m, lifting speed v, and final speed $\omega_m = 0$, $v = 0$. It is assumed that the braking process slows down the speed uniformly. The distance the sliding frame will travel down during deceleration due to braking is deduced from the acceleration formula $a = ds/dt^2$ at the initial conditions $s(0) = 0$ and $ds(0)/dt = 0$.

Calculating the same math for the Figure 2(b) diagram gives:

$$\Delta E = \left(\frac{I_d}{2i_{23}^2} + \frac{I_{g2}}{2i_{23}^2} + \frac{I_{g3} + I_{g4} + I_5}{2}\right)\omega_m^2 - \frac{G_2 v^2}{2g} + \frac{(G_2 + \psi G_1)v^2}{2g} + \frac{\gamma H v^2}{2g} - G_2 s - \frac{\gamma g}{2} s^2 + \frac{\gamma g}{2}[H^2 - (H - s)^2] + (G_2 + \psi G_1)s + W_{ms} s \quad (11)$$

The work done W to brake or stop a mechanical system is in equilibrium with the total energy change ΔE, transformed and calculated by:

$$W = \int_{t_1}^{t_2} (\omega_m - \alpha t) T dt = T(\omega_m - \frac{\alpha t}{2})t = \Delta E \quad (12)$$

where a is the rotation angle of the active brake (rad), t is the braking time, and $t_1 = 0$, $t_2 = t(s)$. In the case of braking, the speed decreases from ω_m to zero. Assuming the braking torque is constant and that the speed when braking is gradually slowing down, the required braking torque T (Nm) is given by:

$$T = \frac{2\Delta E}{(\omega_m + \omega_t)t} = \frac{2\Delta E}{\omega_m t} \quad (13)$$

where ω_t is the angular velocity at the end of braking (rad/s).

C. Test Method

Figure 4 describes the calculation method and numerical experimental procedure, using the established analytical formula to calculate driving power and braking torque, considering the influence of the balancing system.

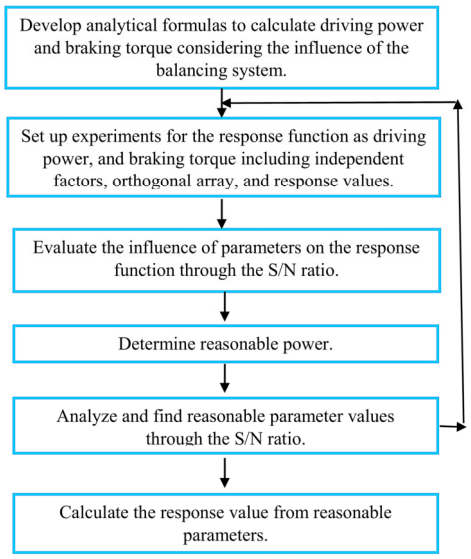

Fig. 4. Computational method and numerical experimental procedure.

Table I shows the factors of the test example. The test parameters include the counterweight, the balance coefficient, the braking time, and the lifting height. Table II shows the survey parameters and value levels. The response functions are driving power N_1, N_2 and braking torque T_1, T_2. The planning matrix is selected according to the Taguchi method and Minitab software. Table III shows the L16 planning matrix used for experimental analysis.

TABLE I. INDEPENDENT PARAMETERS

Parameter	Symbol	Value	Unit
Weight of the car	G_1	25500	N
Weight of sliding frame	G_2	16000	N
Moment of inertia of worm wheel 2	I_{g2}	0.295938	kgm^2
Screw moment of inertia 3	I_{g3}	0.000757	kgm^2
Brake wheel moment of inertia	I_{g4}	0.192668	kgm^2
Engine rotor moment of inertia	I_{g5}	0.082	kgm^2
Moment of inertia of friction drum	I_d	31.462	kgm^2
Cable weight per 1 meter long	γ	3.96	Kg/m
Lifting or lowering speed	v	1	m/s
Gravitational acceleration	g	9.81	m/s^2
Transmission ratio	I_{23}	39.6	
The secondary resistance moves the sliding frame	W_{ms}	2800	N

TABLE II. FACTORS AND VALUE LEVELS

Influential factors	Code	Value level				Range of change
		1	2	3	4	
Balance coefficient ψ	x_1	0.3	0.5	0.7	0.9	0.6
Braking time t, s	x_2	1	2	3	4	3
Lifting height H, m	x_3	10	15	20	25	15

TABLE III. EXPERIMENTAL DESIGN USING L16 ORTHOGONAL ARRAY

N	x_1	x_2	x_3	T_1 (Nm)	T_2 (Nm)	N_1 (kW)	N_2 (kW)
1	1	1	1	158.5	126.5	22.82	5.7
2	1	2	2	131.2	100	23	5.9
3	1	3	3	122.8	92	23.3	6.11
4	1	4	4	119.3	88.5	23.5	6.32
5	2	1	2	122.7	161	17.53	11.45
6	2	2	1	95.6	132.4	17.32	11.23
7	2	3	4	89.4	126.9	18	11.87
8	2	4	3	83.5	120.8	18	11.87
9	3	1	3	87	196.3	12.41	17.2
10	3	2	4	63.1	170	12.41	17.41
11	3	3	1	50.8	156.6	11.78	16.78
12	3	4	2	47.8	153	12	17
13	4	1	4	50	231	6.87	22.96
14	4	2	3	26.5	202	6.66	22.75
15	4	3	2	17.34	191.5	6.66	22.53
16	4	4	1	12	185.5	6.23	22.32

The Signal to Noise (S/N) ratio for the problem is given by:

$$S/N = -10\,lg\left(\frac{1}{n}\sum_{u=1}^{n} Y_{iu}^2\right) \quad (14)$$

where u is the experimental sequence number, n is the number of experiments, and Y_i is the response value $Y_i = N_i$, $Y_i = T_i$. The influence of the parameters was calculated, and the results were analyzed to choose a reasonable value with the response functions. At first, the driving power N_i was calculated. Then, brake torque T_i was calculated and selected according to reasonable driving power parameters.

III. RESULTS AND DISCUSSION

A. Results

The Minitab software was used to calculate and create the graphs. The amount of counterweight G_3, through the balance coefficient ψ, has a decisive influence on the driving power. The driving power in the full-load case N_1 varies inversely with the power in the no-load case N_2 when ψ = 0.3 – 0.9. The reasonable power value in Figure 5 was determined to be N = 14.6 kW, and correspondingly in Figure 6, a reasonable balance coefficient was obtained according to the capacity N = 14.6 kW as ψ = 0.61. ψ was chosen as 0.61 according to the reasonable capacity corresponding to the S/N ratios of -36 (Figure 7) and -43.3 (Figure 8). With the corresponding S/N ratios, the braking time is t = 2 s, and the design lifting height according to the technical requirements H = 18 m. Acceleration is a = 1 m/s^2, and the braking distance when lowering is s = 1 m. Table IV shows the calculation results with the balance coefficients in [14-15], using (1), (2), (13) with ψ = 0.5 and reasonable values, finding that the power decreased by 17.5%, while the braking torque only increased by 13.4%.

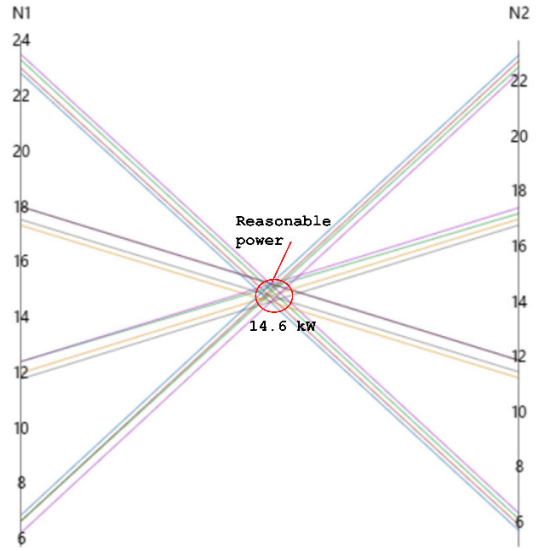

Fig. 5. Determining reasonable power.

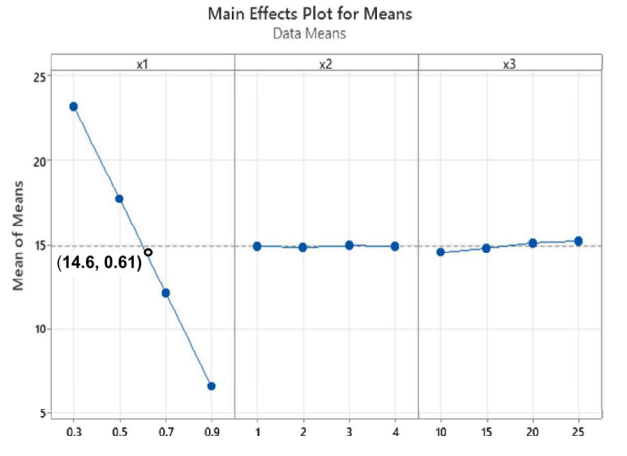

Fig. 6. Influence parameters on driving power N_1.

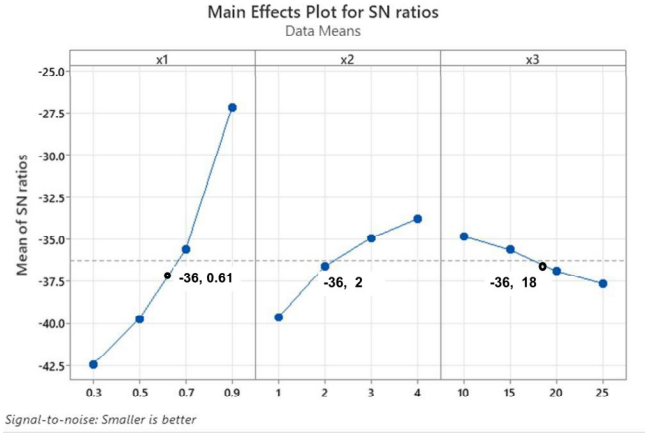

Fig. 7. Analysis of the influence of S/N ratios on braking torque, when braking lowers the fully loaded sliding frame at the bottom.

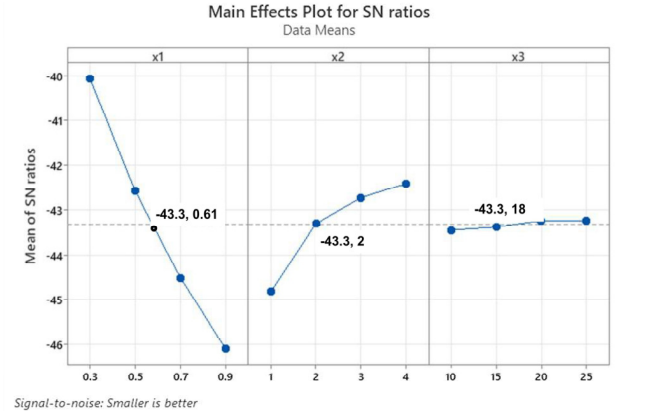

Fig. 8. Analysis of the influence of S/N ratios on braking torque, when braking raises the unloaded sliding frame at the top.

TABLE IV. COMPARISON OF RESPONSE VALUES

Parameter	ψ	N_1 (kW)	N_2 (kW)	T_1 (Nm)	T_2 (Nm)
Choosing according to the usual method	0.5	17.7	11.6	97	134
Reasonable value	0.61	14.6		152	
Compare results	+22%	-17.5%		+13,4%	

B. Discussion

Analyzing the S/N ratio shows that the braking torque is most heavily dependent on the amount of counterweight through the balance coefficient. Then there is the braking time. Lifting height has little effect on power and braking torque. Choosing a reasonable balance coefficient will contribute to saving energy for multi-story parking car systems. The influence of a car's weight on the balance coefficient requires further evaluation. However, the power and braking torque values in this test considered the maximum value of the car weight, so they can meet the working requirements of the elevator. The parameters of the balancing system also affect the traction capacity of the friction drum. The pull capacity of the winch can be adjusted by a reasonable cable groove on the friction drum and the cable embrace angle on the friction drum without changing the balance coefficient.

IV. CONCLUSION

This paper presented a method for determining the weight of the counterweight in a tower car parking system, through the balance coefficient to ensure optimal driving power and established an expression to calculate elevator brake torque, considering the elements of the balanced system. The calculation method to determine the balance coefficient to optimize power and braking torque was based on a planning matrix, Taguchi analysis, and Minitab software. The results of the experimental calculations of the parameters to select an optimal driving power were a balance coefficient $\psi = 0.61$, acceleration $a = 1$ m/s^2, and a braking distance when lowering $s = 1$ m. Compared to the conventional method where $\psi = 0.5$, the power was reduced by 17.5% and the braking torque was increased by 13.4%. Choosing a reasonable balance coefficient will contribute to saving energy for multi-story car parking systems. The braking torque depends most heavily on the amount of counterweight through the balance coefficient. Then there is the braking time. Lifting height has little effect on power and braking torque. Future research would be to apply this calculation method to investigate the pull capacity of the winch.

ACKNOWLEDGMENT

The author would like to thank the Hanoi University of Civil Engineering for allowing conducting this research.

REFERENCES

[1] S. S. Ali and A. H. K. Albayati, "Statistical Modeling for Traffic Noise: The Case of Kirkuk City," *Engineering, Technology & Applied Science Research*, vol. 12, no. 5, pp. 9108–9112, Oct. 2022, https://doi.org/10.48084/etasr.5173.

[2] A. Skrzyniowski, A. Mruk, and D. Skrzyniowska, "Rotary Smart Car Parking System," *Technical Transactions*, vol. 115, no. 3, pp. 211–227, Mar. 2018, https://doi.org/10.4467/2353737XCT.18.049.8344.

[3] N. H. Patel, "Review on Different Types of Car Parking Systems," *International Journal for Research in Emerging Science and Technology*, vol. 7, no. 5, May 2020.

[4] T. G. Duong, "Research on parameters to evaluation, selection storage solutions of multilevel car parking," *Journal of Science and Technology in Civil Engineering*, vol. 10, no. 1, pp. 8–16, Jan. 2016.

[5] J. Filas and M. Mudroň, "The Dynamic Equation of Motion of Driving Mechanism of a Freight Elevator," *Procedia Engineering*, vol. 48, pp. 149–152, Jan. 2012, https://doi.org/10.1016/j.proeng.2012.09.498.

[6] J. Vladić, R. Đokić, and H. Ličen, "Dynamic analysis of load lifting machines and correlation with measurement results," *Research & Development in Heavy Machinery*, vol. 21, no. 4, pp. 35–40, 2015, https://doi.org/10.5937/IMK1502035V.

[7] S. Mikšíková, D. Ulčák, and F. Kuda, "Analysis of Malfunctions in Selected Parking Systems in the Czech Republic," *Sustainability*, vol. 14, no. 3, Art. no. 1826, Jan. 2022, https://doi.org/10.3390/su14031826.

[8] P. L. Chang and C. F. Chang, "Mechanical parking garage," US10794077B1, Oct. 06, 2020.

[9] M. U. Artamonov, "Modular multistorey robotized car park," US20130078062A1, Mar. 28, 2013.

[10] S. I. Belinsky, "High-rise automated garage," US5893696A, Apr. 13, 1999.

[11] T. I. Chen, "Multi-storey parking garage," US20050281640A1, Dec. 22, 2005.

[12] L. Hrabovský, "Forces Generated in the Parking Brake of the Pallet Locking System," *Advances in Science and Technology Research Journal*, vol. 13, no. 4, pp. 181–187, Dec. 2019, https://doi.org/10.12913/22998624/111478.

[13] T. Tyni and P. Perala, "Method for determining the weight of the car and counterweight in an elevator," EP3538465B1, Apr. 05, 2023.

[14] S. Feng, Y. Liang, J. Chen, and K. Niu, "Design of Weight Cart for Elevator Balance Coefficient Test," in *Proceedings of the 2022 2nd International Conference on Control and Intelligent Robotics*, Nanjing, China, Jul. 2022, pp. 442–444, https://doi.org/10.1145/3548608.3559238.

[15] T. Q. Thanh and P. Q. Dung, *Lifting machines and equipment*. Vietnam: Scientific and Technical Publishing, 2004.

[16] B. T. Danh and N. V. Cuong, "Surface Roughness Modeling of Hard Turning 080A67 Steel," *Engineering, Technology & Applied Science Research*, vol. 13, no. 3, pp. 10659–10663, Jun. 2023, https://doi.org/10.48084/etasr.5790.

[17] T. G. Duong, "Determining parameters to optimize the pulling force for the luffing jib tower cranes by Taguchi method," *Archive of Mechanical Engineering*, vol. 70, no. 3, pp. 387–407, 2023, https://doi.org/10.24425/ame.2023.146845.

[18] D. T. Giang, "Study to Determine the Effect of Blade Distance and Chain Speed on the Productivity of Trench Excavators Using Taguchi Method," *Advances in Science and Technology Research Journal*, vol. 17, no. 4, pp. 139–149, Aug. 2023, https://doi.org/10.12913/22998624/169427.

[19] A. Alzahougi, B. Demir, and M. Elitas, "An Optimization Study on Resistance Spot Welding of DP600 Sheet Steel via Experiment and Statistical Analysis," *Engineering, Technology & Applied Science Research*, vol. 13, no. 4, pp. 11106–11111, Aug. 2023, https://doi.org/10.48084/etasr.5804.